Kuwait Journal of Science 54 (2027) 100699

Contents lists available at ScienceDirect

Kuwait Journal of Science

journal homepage: www.sciencedirect.com/journal/kuwait-journal-of-science

Full Length Article

Attenuation of cisplatin-induced oxidative ovarian injury by usnic acid in rats through inhibition of inflammation and endoplasmic reticulum stress

Selim Demir [a,*], Nihal Turkmen Alemdar [b], Ayten Livaoglu [c], Elif Ayazoglu Demir [d], Huseyin Yaman [a], Ahmet Mentese [a], Yuksel Aliyazicioglu [a]

[a] Department of Medical Biochemistry, Faculty of Medicine, Karadeniz Technical University, Trabzon, 61080, Türkiye
[b] Department of Medical Services and Techniques, Vocational School of Health Services, Recep Tayyip Erdogan University, Rize, 53100, Türkiye
[c] Department of Medical Pathology, Faculty of Medicine, Trabzon University, Trabzon, 61250, Türkiye
[d] Department of Chemistry and Chemical Processing Technologies, Macka Vocational School, Karadeniz Technical University, Trabzon, 61750, Türkiye

ARTICLE INFO

Keywords:
Apoptosis
Cisplatin
ER stress
Inflammation
Nrf2
Oxidative stress
Ovotoxicity
Usnic acid

ABSTRACT

Despite its effectiveness as a DNA intercalator in the treatment of numerous cancers, cisplatin (CIS) exerts deleterious effects on healthy cells, including those that function in reproductive organs. Usnic acid (UA) is a dibenzofuran derivative that is naturally present in lichens and is widely employed in traditional medicine on account of its antioxidant and analgesic activity. The current study aimed to evaluate the therapeutic potential of UA in counteracting CIS-induced ovotoxicity. The experiments comprised five groups of 6 rats each, which were categorised as follows: control, UA (10 mg/kg), CIS (5 mg/kg), CIS + UAs (5 and 10 mg/kg). Subsequent to the conclusion of the experimental procedures, the serum and ovarian tissues collected were subjected to biochemical and histopathological analysis. The results revealed that the CIS administration led to the suppression of the antioxidant system, which resulted from the depletion of the reduced glutathione (GSH) pool within the ovarian tissue. Furthermore, the administration of CIS was found to induce lipid peroxidation (LPO), inflammation, and endoplasmic reticulum stress (ERS). Conversely, UA treatments following CIS administration led to a substantial reduction in LPO levels by means of regeneration of the intracellular GSH pool. Furthermore, the administration of UA treatments resulted in the suppression of inflammatory and ERS processes, which was achieved via modulation of the Nrf2 pathway. Furthermore, the chemoprotective potential of UA was confirmed by serum anti-mullerian hormone levels and histological analysis. Consequently, UA may be considered as a potential chemotherapy-supporting molecule that can protect ovarian tissue following CIS chemotherapy.

1. Introduction

Cancer continues to be a major cause of mortality worldwide; however, progress in treatment protocols has led to a 20% increase in survival rates over the past three decades (Bhardwaj et al., 2023). Although the implementation of chemotherapy protocols has been identified as a significant factor contributing to enhanced survival rates, further investigation is necessary to ascertain efficacious remedies for the toxicity patterns that have been observed, particularly those that impact the reproductive system (Morgan et al., 2012). Cisplatin (CIS) has been used globally since 1978 as a pharmaceutical agent against various malignancies, including testicular, ovarian, breast, lung and bladder cancers (Bhardwaj et al., 2023). The classical anticancer mechanism of action of CIS is based on the intercalation into the DNA of cancer cells and the inhibition of replication by DNA adducts formed by intra- and inter-strand interactions (Dasari and Tchounwou, 2014). New information has also emerged indicating that CIS accelerates the process of apoptosis in cancer cells by increasing the production of reactive oxygen species (ROS) within the cell (Zhou et al., 2022). It is unfortunate that the clinical application of CIS is limited by various side effects, including neuro-, nephro-, oto- and ovotoxicity (Mashayekhi-Sardoo et al., 2025). The ovary is one of the organs most adversely affected by the toxicity of CIS, and the CIS chemotherapy causes ovarian damage, decreased follicular reserve, premature ovarian failure and menopause, thus reducing female fertility potential (Bhardwaj et al., 2023). Intracellular stress responses, including oxidative stress (OS), mitochondrial dysfunction, endoplasmic reticulum stress (ERS), inflammation, and apoptosis, have been demonstrated to contribute to the toxicity of CIS

* Corresponding author.
E-mail addresses: selim-demir@hotmail.com, selim.demir@ktu.edu.tr (S. Demir).

https://doi.org/10.1016/j.kjs.2026.100699
Received 2 December 2025; Received in revised form 29 September 2026; Accepted 30 September 2026
Available online 30 September 2026
2307-4108/© 2026 The Authors. Published by Elsevier B.V. on behalf of Kuwait University. This is an open access article under the CC BY license (http://creativecommons.org/licenses/by/4.0/).

(Zhou et al., 2022; Mashayekhi-Sardoo et al., 2025). CIS-induced ovotoxicity is primarily characterised by a rise in intracellular ROS levels, which, in turn, results in the consumption of the reduced glutathione (GSH) pool, the inhibition of the antioxidant system, including superoxide dismutase (SOD) and glutathione peroxidase (GPx) and, ultimately, cell damage via the process of lipid peroxidation (LPO) (Bhardwaj et al., 2023). Furthermore, the increased OS has been observed to cause ovarian dysfunction, characterised by structural degeneration of ovarian tissue and a decline in the level of anti-mullerian hormone (AMH) secretion by granulosa cells, which is responsible for the maturation of the ovaries (Özcan et al., 2015; Ayazoglu Demir et al., 2023). Secondly, the increase in ROS caused by CIS activates nuclear factor-kappa B (NF-κB) signalling, a pivotal regulator of cellular inflammation. This, in turn, further exacerbates existing damage by increasing pro-inflammatory tumor necrosis factor-alpha (TNF-α) levels and leukocyte infiltration into damaged tissue (which is characterised by higher myeloperoxidase (MPO) levels) (Zhou et al., 2022). Thirdly, CIS has been demonstrated to induce a decline in the expression of glycolysis pathway enzymes, including phosphofructokinase-1, within the cells, consequently resulting in a decrease in cellular ATP levels (Raudenska et al., 2019). The heightened OS, inflammation, and exhausted ATP levels collectively diminish the protein folding potential of ER, culminating in ERS and this complex process ultimately results in apoptosis (Mashayekhi-Sardoo et al., 2025). Nuclear factor erythroid 2-related factor 2 (Nrf2), a redox-sensitive transcription, has been identified as a master regulator of cytoprotective genes, including SOD, GPx and heme-oxygenase 1 (HO-1) (Ebrahimi et al., 2025). Recent research has indicated that the inhibition of the CIS-induced Nrf2 pathway contributes to CIS toxicity (Zhou et al., 2022; Mashayekhi-Sardoo et al., 2025). The research interest has therefore focused on the antioxidant and Nrf2 modulatory activities of secondary metabolites found in natural products, and their protective potential against CIS-induced toxicities (Huang et al., 2023).

Lichens are defined as organisms that arise from the symbiotic relationship between a fungal component (mycobiont) and a photosynthetic algae or cyanobacteria (photobiont) (Zhao et al., 2021). This symbiosis gives rise to a greater variety of secondary metabolites than is observed in other natural products (Calcott et al., 2018). Usnic acid (UA), a dibenzofuran derivative, is a particularly intriguing secondary lichen metabolite which has been found in higher concentrations in genera such as *Usnea*, *Lecanora,* and *Flavocetraria* (Paździora et al., 2023). A growing body of research has identified that UA has antimicrobial, anti-inflammatory, and antioxidant properties (Calcott et al., 2018). Its use in wound and ulcer treatments is well-documented, and it has seen increased application in the pharmaceutical and cosmetic industries (Zhao et al., 2021; Demir et al., 2024a). As demonstrated previously, the tissue protective effects of UA have been shown in models of indomethacin-induced gastric (Odabasoglu et al., 2006) and methotrexate-induced lung injuries (Demir et al., 2025) models. However, the question of whether UA has the capacity to exert a protective effect against toxicity in organs related to CIS remains unanswered. The current study therefore sought to evaluate the chemoprotective potential of UA in the CIS-induced ovotoxicity model by incorporating Nrf2 signalling pathway analysis at both biochemical and histological levels.

2. Materials and methods

2.1. Animals

The experiments were conducted using 30 adult female Sprague-Dawley rats, with a mean weight of approximately 185-195 g. The animals were housed at a constant temperature of 25°C and under a 12-h light/dark cycle, and food and water were provided *ad libitum*. All procedures for animal experimentation were approved by the Animal Research Ethic Committee of Karadeniz Technical University (Approval number: 2021/48) and conducted precisely according to the Directive 2010/63/EU and ARRIVE guideline.

2.2. Preparation of UA and CIS

CIS and UA were procured from Sigma-Aldrich (St. Louis, MO, USA) and prepared by dissolution in sterile physiological saline (Mohamed et al., 2020) and 10% dimethyl sulfoxide (DMSO) (Demir et al., 2025), respectively.

2.3. Establishment of CIS-induced ovotoxicity model and UA treatments

Only rats that were determined to be in oestrus by vaginal smear were included in the study (Mentese et al., 2022) and randomly assigned to one of five groups: vehicle control, CIS, CIS + UAs (5 and 10 mg/kg) and UA (10 mg/kg). The CIS-induced ovotoxicity model was established on the first day of the experiment with a single intraperitoneal CIS (5 mg/kg) injection, taking into account previous reports (Aksoy et al., 2015; Ayazoglu Demir, 2024). Groups designated as CIS-free were administered a sterile physiological saline injection on the first day of the experiment. Subsequent to the administration of CIS applications, UA applications (5 and 10 mg/kg) were administered intraperitoneally over a period of three consecutive days. Groups designated as UA-free received 10% DMSO injections on the same days. The UA doses utilised in the present study were established on the basis of preceding experimental investigations in which UA was demonstrated to possess anti-inflammatory and chemopreventive properties (Lee et al., 2020; Demir et al., 2025). Twenty-four hours after the final injection (on day 5), the animals were sacrificed by spinal dislocation while under general anaesthesia involving ketamine (60 mg/kg) and xylazine (10 mg/kg), after which the ovarian tissues were swiftly removed. Samples of blood were taken from the heart using a needle and put into serum separation tubes that can separate the blood. The ovarian samples were divided into two parts, one for biochemical analysis and the other for histological examination.

2.4. Tissue processing and protein determination

The ovarian tissues of rats underwent a series of processing steps, including rinsing, slicing, and homogenisation in cold phosphate buffered saline at a weight-to-volume ratio of 1:9. The homogenates were then subjected to a centrifugation process (1800 g/15 min) at a temperature of 4°C. The bicinchoninic acid method was utilised to determine the protein concentration of the obtained supernatants (Smith et al., 1985).

2.5. Measurement of OS biomarkers

The tissue levels of LPO were established using a previously outlined colorimetric approach to measure malondialdehyde (MDA) (Mihara and Uchiyama, 1978). The colour formation resulting from the reaction between MDA and thiobarbituric acid was measured at 532 nm using a spectrophotometer (Molecular Devices, CA, USA) and the results were expressed as nmol/mg protein (Yuluğ et al., 2019). The determination of SOD, GSH, GPx, Nrf2, HO-1 and NAD(P)H:quinone oxidoreductase-1 (NQO-1) tissue levels was conducted using enzyme-linked immunosorbent assay (ELISA) kits purchased from Finetest (Wuhan, China). The determination of total oxidant status (TOS) tissue levels was conducted using a colorimetric kit purchased from Rel Assay Diagnostics (Gaziantep, Türkiye) and the results were expressed as μmol H_2O_2 equivalent/L (Mentese et al., 2014). All procedures were performed in accordance with the manufacturer's instructions (n = 6 for each group). The following summary steps were followed for a classical ELISA procedure: 100 µL of standard solutions, prepared by serial dilution, and of the supernatant were added to the 96-well microplate, which was coated with a specific antibody. After a 90-min incubation at 37°C, the contents of each well were removed and a biotin-labelled detection antibody was

added. After a further 60-min incubation at 37°C, the contents of the wells were removed and an HRP-conjugated antibody solution was added to each well. After a further 30-min incubation at 37°C, the contents of each well were removed and a substrate solution was added. After a further 20-min incubation at 37°C, stop solution was added to each well, after which the absorbance of the resulting yellow colour was measured at 450 nm using a spectrophotometer. The amount of analyte was determined using the absorbance of the samples, as plotted in the graph, which was created using the absorbance and concentrations of the standard solutions (Ayazoglu Demir, 2024).

2.6. Measurement of inflammation biomarkers

The quantification of ovarian inflammation markers (high-mobility group box 1 (HMGB1), NF-κB p65, TNF-α, and MPO) were conducted through the utilisation of ELISA kits (Finetest, Wuhan, China). The measurement of samples absorbance was determined by means of a microplate reader (Molecular Devices, CA, USA) (n = 6 for each group).

2.7. Measurement of ERS and apoptosis biomarkers

The quantification of ovarian ERS [binding immunoglobulin protein (BİP), activating transcription factor 6 (ATF6), growth arrest and DNA damage-inducible gene 153 (GADD153)] and apoptosis [B cell lymphoma 2 (Bcl-2), Bcl-2-like protein 4 (Bax) and caspase-3 (CASP3)] markers were conducted through the utilisation of ELISA kits (Finetest, Wuhan, China). All procedures were performed in accordance with the manufacturer's instructions (n = 6 for each group).

2.8. Measurement of serum AMH levels

The determination of AMH serum levels was conducted using an ELISA kit purchased from Finetest (Wuhan, China). All procedures were performed in accordance with the manufacturer's instructions (n = 6 for each group). Results were presented as pg/mL.

2.9. Histological examination of ovarian tissues

The ovarian tissues were fixed in 10% neutral buffered formalin, cut, washed, and dehydrated in a series of increasing concentrations of alcohol. The specimens were then cleared in xylene and embedded in paraffin wax. Five-micrometre sections obtained from paraffin blocks were stained with hematoxylin and eosin, examined under a light microscope and photographed by an investigator unaware of the experimental history of the groups (Kaygusuzoglu et al., 2018). Furthermore, the presence of pathological findings in each preparation was evaluated using a semi-quantitative scale, where 0 represented 'not at all' and 3 indicated 'very common' (Ayazoglu Demir, 2024).

2.10. Statistical analysis

Data were expressed as mean ± SEM. Statistical analysis of the data was analyzed using SPSS 23.0 software. Differences between groups were determined with one-way ANOVA and post-hoc Tukey tests. P values < 0.05 were considered statistically significant.

3. Results

3.1. UA inhibited OS process in CIS-intoxicated rats

As shown in Table 1, the levels of TOS and MDA increased significantly in rat ovaries to which CIS had been applied, due to an increase in ROS. Meanwhile, the antioxidant defence line consisting of GSH, SOD, and GPx was significantly inhibited. Although the low-dose UA (5 mg/kg) treatment group showed significant improvements in LPO and TOS levels compared to the CIS group, this was insufficient to support the antioxidant system. By contrast, high-dose UA (10 mg/kg) treatment was found to significantly regenerate the antioxidant system, while also suppressing elevated LPO and TOS levels compared to the CIS group. In addition, alone high-dose UA treatment did not cause any oxidative injury in comparison to the control group.

3.2. UA modulated Nrf2 signaling in CIS-intoxicated rats

The rats that had been treated with CIS exhibited a marked diminution in Nrf2, HO-1, and NQO-1 levels in ovarian tissue in comparison to control rats (Fig. 1). Interestingly, low-dose UA treatment significantly improved only NQO-1 levels in CIS-induced Nrf2 pathway inhibition, while high-dose UA treatment regenerated all components of Nrf2 signalling.

3.3. UA suppressed inflammatory process in CIS-intoxicated rats

The levels of tissue inflammation markers for all the groups were shown in Fig. 2. The results showed that CIS injection exacerbated inflammation in the rat ovary. In contrast, CIS-induced inflammation was significantly suppressed by treatment with UA, especially at a dose of 10 mg/kg. In addition, a high-dose UA treatment alone did not cause any inflammatory processes in comparison to the control group.

3.4. UA alleviated ERS and apoptosis in CIS-intoxicated rats

As shown in Table 2, the levels of all ERS and apoptosis biomarkers were significantly higher in the ovaries of CIS-treated rats than in the ovaries of control rats. Interestingly, UA treatment significantly reduced ERS and apoptosis levels in a dose-dependent manner, compared with rats that received only CIS. In addition, a high-dose UA treatment alone did not cause any pathological findings in terms of ERS and apoptosis in comparison to the control group.

3.5. UA restored histolopathological architecture and serum AMH levels in CIS-intoxicated rats

Fig. 3 shows the histopathological changes observed in ovarian tissue in all groups, and Table 3 shows the serum AMH levels and semi-quantitative histopathological scores for the groups. Normal ovarian histology findings were obtained in both the control group (Fig. 3A) and the group that received high-dose UA treatment alone (Fig. 3E). The CIS

Table 1
Effects of UA (5 and 10 mg/kg, i.p) on ovarian oxidant and antioxidant parameters of CIS-induced injury in rats.

	Control	UA (10 mg/kg)	CIS	CIS + UA (5 mg/kg)	CIS + UA (10 mg/kg)
MDA (nmol/mg protein)	71.6 ± 10.8	70.3 ± 10.7	593.9 ± 105.8$^{\#\#\#}$	189.9 ± 22.9***	76.9 ± 4.8***
TOS (μmol H_2O_2 equi/L)	19.2 ± 0.4	18.4 ± 0.5	85.5 ± 8.4$^{\#\#\#}$	44.7 ± 11.9**	20.8 ± 1.9***
SOD (ng/mg protein)	6.8 ± 0.6	6.9 ± 1.0	1.6 ± 0.2$^{\#\#\#}$	4.0 ± 0.4	7.0 ± 1.0***
GPx (pg/mg protein)	535.0 ± 85.4	562.9 ± 53.5	147.5 ± 28.0$^{\#}$	313.6 ± 42.2	534.0 ± 131.4*
GSH (μg/mg protein)	50.9 ± 5.1	56.2 ± 6.5	16.0 ± 2.8$^{\#}$	34.3 ± 3.9	52.5 ± 16.4*

Data represented as mean ± SEM (n = 6). P-values according to one-way ANOVA test, post-hoc Tukey test. $^{\#}p < 0.05$, $^{\#\#\#}p < 0.001$ *vs.* control group. *p < 0.05, **p < 0.01, ***p < 0.001 *vs.* CIS group. CIS; cisplatin, GPx; glutathione peroxidase, GSH; glutathione, MDA; malondialdehyde, SOD; superoxide dismutase, TOS; total oxidant status, UA: usnic acid.

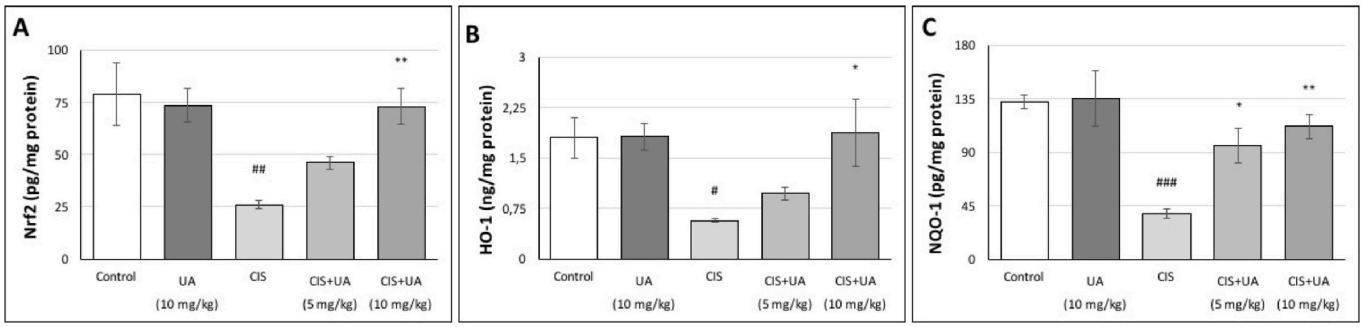


Fig. 1. Effects of UA (5 and 10 mg/kg, i.p) on ovarian (A) Nrf2, (B) HO-1 and (C) NQO-1 levels of CIS-induced injury in rats. Data represented as mean ± SEM (n = 6). P-values according to one-way ANOVA test, post-hoc Tukey test. $^{\#}p < 0.05$, $^{\#\#}p < 0.01$, $^{\#\#\#}p < 0.001$ *vs.* control group. *p < 0.05, **p < 0.01 *vs.* CIS group. CIS; cisplatin, HO-1; heme oxygenase-1, Nrf2; nuclear factor erythroid 2-related factor 2, NQO-1; NAD(P)H:quinone oxidoreductase-1, UA; usnic acid.

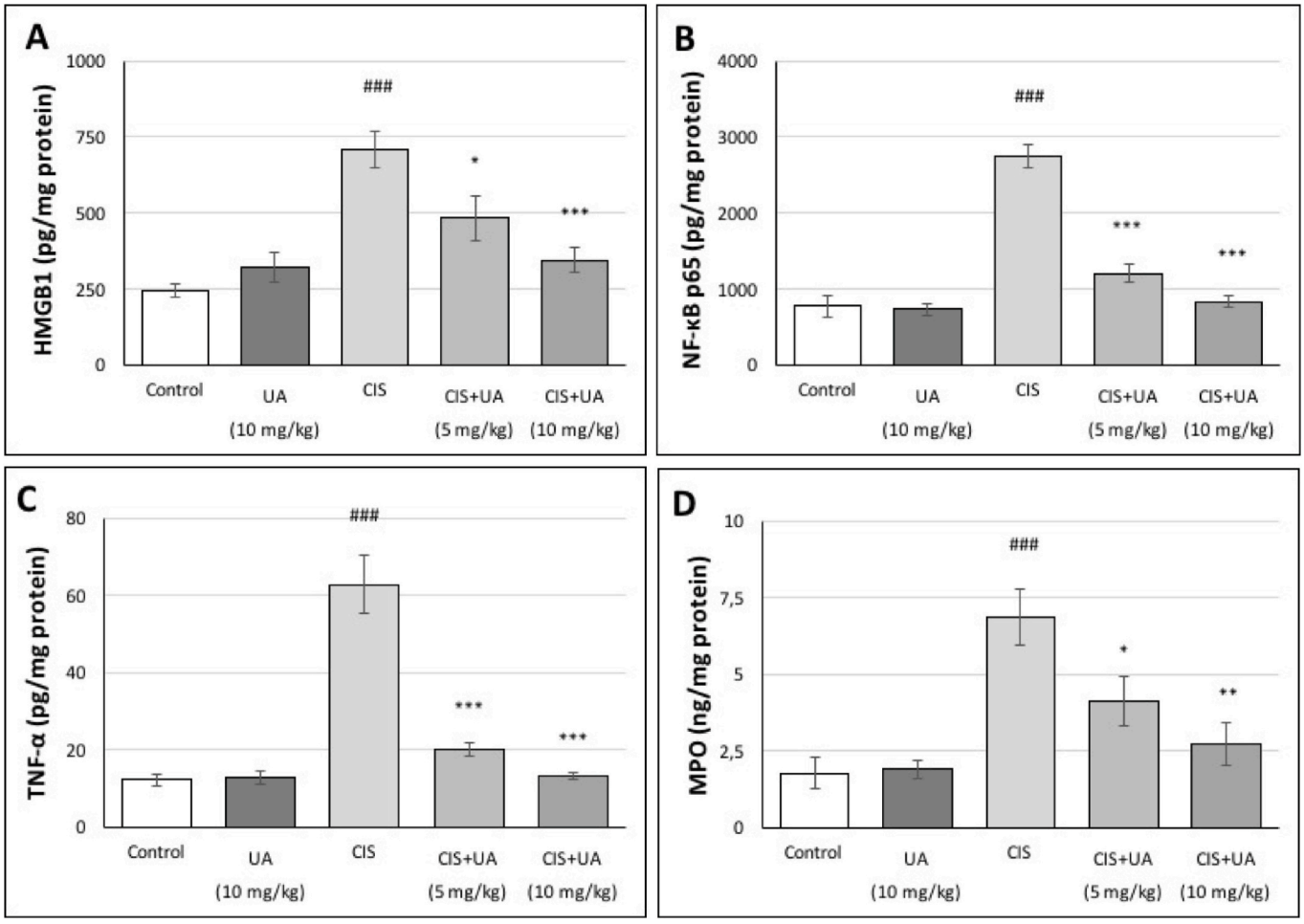


Fig. 2. Effects of UA (5 and 10 mg/kg, i.p) on ovarian (A) HMGB1, (B) NF-κB p65, (C) TNF-α and (D) MPO levels of CIS-induced injury in rats. Data represented as mean ± SEM (n = 6). P-values according to one-way ANOVA test, post-hoc Tukey test. $^{\#\#\#}p < 0.001$ *vs.* control group. *p < 0.05, **p < 0.01, ***p < 0.001 *vs.* CIS group. CIS; cisplatin, HMGB1; high-mobility group box 1, MPO; myeloperoxidase, NF-κB p65; nuclear factor kappa B protein 65, TNF-α; tumor necrosis factor-alpha, UA; usnic acid.

group exhibited severe congestion and edema, characterised by degenerated ovarian architecture (Fig. 3B) and dramatically decreased serum AMH levels (Table 3). By contrast, UA treatments (particularly at a dose of 10 mg/kg) largely restored histopathological findings (Fig. 3C and D) and serum AMH levels compared to the CIS group (Table 3).

4. Discussion

Despite the wide use of CIS in cancer chemotherapy, the determination of its ovotoxic effects poses a significant risk to the fertility of young female individuals (Bhardwaj et al., 2023). Therefore, in recent years, researchers have conducted many studies investigating the protective/therapeutic properties of many natural compounds, such as resveratrol (Özcan et al., 2015), syringic acid (Ayazoglu Demir, 2024), zingerone (Kaygusuzoglu et al., 2018) and icariin (Li et al., 2024) against CIS-induced ovotoxicity. The strong antioxidant effects of UA, a lichen metabolite, have been exhibited in experimental models of indomethacin-induced gastric (Odabasoglu et al., 2006) and

Table 2
Effects of UA (5 and 10 mg/kg, i.p) on ovarian ERS and apoptosis parameters of CIS-induced injury in rats.

	Control	UA (10 mg/kg)	CIS	CIS + UA (5 mg/kg)	CIS + UA (10 mg/kg)
BİP (ng/mg protein)	4.5 ± 1.3	4.1 ± 0.4	8.9 ± 1.1$^{\#\#}$	6.3 ± 0.7	4.4 ± 0.4**
ATF6 (pg/mg protein)	339.6 ± 42.1	358.3 ± 47.9	775.6 ± 99.9$^{\#\#}$	692.2 ± 104.4$^{\#}$	383.6 ± 48.2**,^{w}
GADD153 (ng/mg protein)	1.3 ± 0.2	1.2 ± 0.2	9.8 ± 1.4$^{\#\#\#}$	3.4 ± 1.2***	1.4 ± 0.6***
Bax (ng/mg protein)	3.7 ± 0.4	3.5 ± 0.5	8.2 ± 0.9$^{\#\#\#}$	4.7 ± 0.3**	3.8 ± 0.4***
Bcl-2 (ng/mg protein)	1.5 ± 0.2	1.5 ± 0.2	0.4 ± 0.1$^{\#\#}$	0.5 ± 0.1$^{\#\#}$	1.4 ± 0.3**,^{ww}
Bax/Bcl-2 ratio	2.5 ± 0.1	2.5 ± 0.5	24.2 ± 3.7$^{\#\#\#}$	9.4 ± 0.8***	3.4 ± 0.7***
CASP3 (ng/mg protein)	1.1 ± 0.1	1.3 ± 0.1	4.2 ± 0.3$^{\#\#\#}$	2.2 ± 0.1$^{\#\#}$,***	1.4 ± 0.2***,^{w}

Data represented as mean ± SEM (n = 6). P-values according to one-way ANOVA test, post-hoc Tukey test. $^{\#}p < 0.05$, $^{\#\#}p < 0.01$, $^{\#\#\#}p < 0.001$ *vs.* control group. **p < 0.01, ***p < 0.001 *vs.* CIS group. $^{w}p < 0.05$, $^{ww}p<0.01$ *vs.* CIS + UA (5 mg/kg) group. ATF6; activating transcription factor 6, Bax; Bcl-2-like protein 4, Bcl-2; B-cell lymphoma 2, BİP; binding immunoglobulin protein, CASP3; cleaved caspase-3, CIS; cisplatin, GADD153; growth arrest and DNA damage-inducible gene 153, UA; usnic acid.

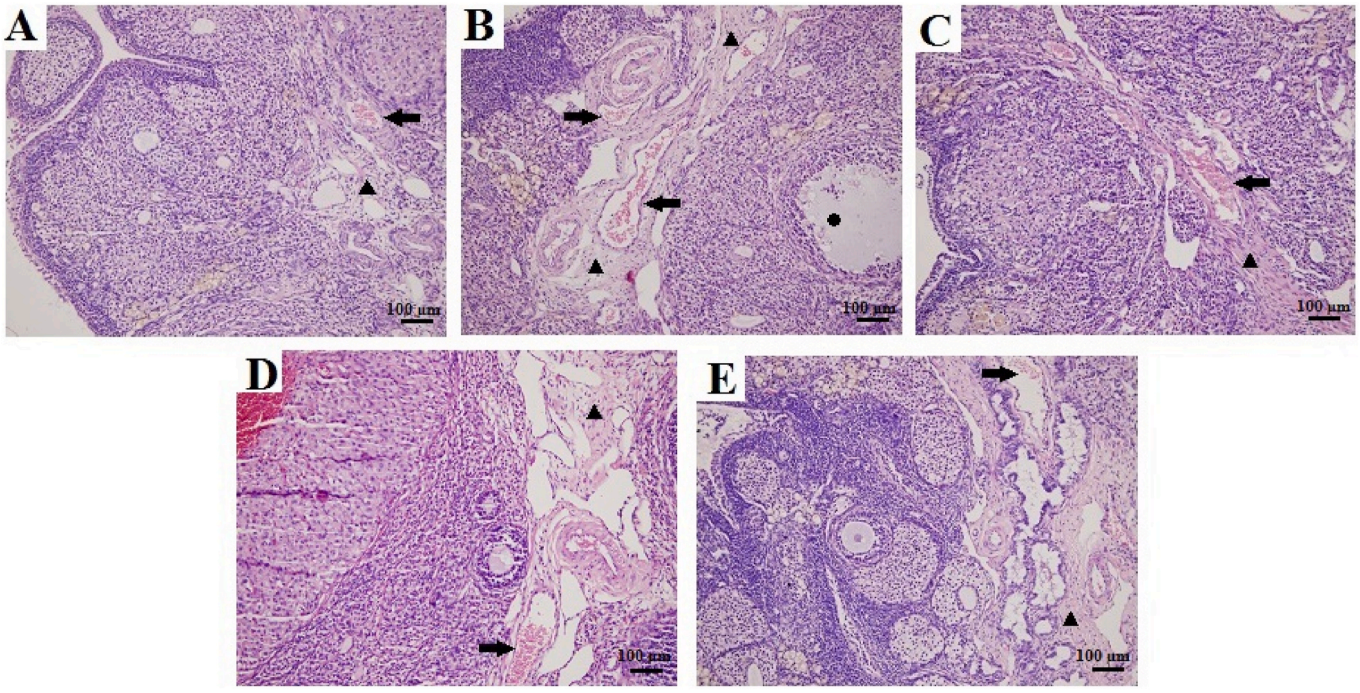


Fig. 3. Histological examination of rat ovarian tissues. CIS; cisplatin, UA; usnic acid. **(A) Control group:** Normal ovarian tissue with mild vascular congestion (black arrow) and edema (filled triangle) in the interstitial area. **(B) CIS group:** Ovarian tissue containing severe vascular congestion (black arrow), edema (filled triangle) and degenerate follicle structure containing pycnotic nuclei and leukocyte infiltration (filled circle) in the interstitial space. **(C) CIS + UA (5 mg/kg) group:** Ovarian tissue containing moderate vascular congestion (black arrow) and edema (filled triangle) in the interstitial area was observed. **(D) CIS + UA (10 mg/kg) group:** An ovarian tissue structure very similar to the control group with mild vascular congestion (black arrow) and edema (filled triangle) in the interstitial area. **(E) UA (10 mg/kg, *per se*) group:** A normal ovarian tissue structure with mild vascular congestion (black arrow) and edema (filled triangle) in the interstitial area.

Table 3
Histopathological scores and serum AMH levels of all groups.

	Control	UA (10 mg/kg)	CIS	CIS + UA (5 mg/kg)	CIS + UA (10 mg/kg)
Vascular congestion	0.33 ± 0.21	0.50 ± 0.22	2.33 ± 0.21$^{\#\#\#}$	1.50 ± 0.22$^{\#}$	0.83 ± 0.40**
Edema	0.33 ± 0.21	0.50 ± 0.22	2.33 ± 0.21$^{\#\#\#}$	1.33 ± 0.21	0.83 ± 0.40**
Hemorrhage	0.00 ± 0.00	0.00 ± 0.00	0.50 ± 0.22	0.33 ± 0.21	0.17 ± 0.17
Follicular degeneration	0.00 ± 0.00	0.00 ± 0.00	0.67 ± 0.21$^{\#}$	0.33 ± 0.21	0.17 ± 0.17
Leukocyte infiltration	0.00 ± 0.00	0.00 ± 0.00	0.67 ± 0.21$^{\#}$	0.17 ± 0.17	0.17 ± 0.17
AMH (pg/mL)	1789.7 ± 263.5	1903.1 ± 171.5	388.8 ± 65.8$^{\#\#\#}$	972.1 ± 212.4$^{\#}$,*	1798.9 ± 226.7***

Data represented as mean ± SEM (n = 6). P-values according to one-way ANOVA test, post-hoc Tukey test. $^{\#}p < 0.05$, $^{\#\#}p < 0.01$ *vs.* control group. *p < 0.05, **p < 0.01, ***p < 0.001 *vs.* CIS group. AMH; anti-mullerian hormone, CIS; cisplatin, UA; usnic acid.

methotrexate-induced lung injury (Demir et al., 2025), with protective effects being demonstrated. However, the potential beneficial pharmacological effects of UA in combatting CIS-induced ovotoxicity remain unclear. This study questioned the hypothesis that UA may have a chemopreventive effect in an experimental CIS ovotoxicity model for the first time. The results showed that UA inhibited OS, inflammation and ERS processes by modulating the Nrf2 pathway. UA was also found to reverse the histopathological architecture in ovarian tissue and the depletion in serum AMH levels. To our knowledge, this is the first study of its kind to explore the chemopreventive effect and potential

mechanisms of UA against CIS-associated ovotoxicity (Fig. 4).

In this investigation, a CIS ovotoxicity prototype was generated in female rats with a single injection of CIS at a dosage of 5 mg/kg, taking into account earlier reports (Aksoy et al., 2015; Ayazoglu Demir, 2024). According to the results that were obtained, in the groups that received only CIS, significant disruption to normal histological architecture was seen and a significant reduction in serum AMH levels, which are considered an indicator of follicular reserve, was recorded. These findings, which are consistent with previous reports (Özcan et al., 2015; Kaygusuzoglu et al., 2018; Ayazoglu Demir, 2024), were evaluated as substantiating evidence that the ovotoxicity model had been effectively established. By contrast, treatment with UA, particularly at a dose of 10 mg/kg following CIS, largely offset the histopathological findings and restored serum AMH levels. Similar results were also observed in previous models, in which UA treatment was found to have protective effects on lung and testicular tissues (Fernández-Moriano et al., 2017; Demir et al., 2024a). AMH is a dimeric protein produced by small, growing follicles, and plasma AMH levels are a more sensitive indirect indicator of ovarian reserve than other hormones because they do not change with the phases of the menstrual cycle (Atli et al., 2017). The impact of CIS on the ovary has been demonstrated to manifest in a series of adverse effects, including ovarian failure, augmented follicular apoptosis, diminished AMH secretion, alterations in the estrous cycle, and a reduction in the number of AMH-producing follicles (Borovskaya et al., 2004; Yeh et al., 2006; Demir et al., 2024b). Therefore, in chemotherapy-induced ovarian damage, the effects of protective molecules are evaluated along with plasma levels of hormones, such as FSH, estradiol, inhibin B, and AMH, as well as follicle morphology (primary, secondary, and antral follicles) (Muttukrishna et al., 2005; Atli et al., 2017). In this study, plasma AMH levels were evaluated using semi-quantitative histopathological scores. However, comprehensive studies of fertility-responsible hormones and follicle morphology should be investigated in future studies.

The OS occurs when the amount of ROS formed in cells exceeds the intracellular antioxidant capacity. It is the most widely studied biochemical mechanism for explaining the toxic effects of CIS (Bhardwaj et al., 2023). The increase in ROS caused by CIS initiates LPO and accelerates the formation of unstable, antigenic intermediates, such as MDA (Dasari and Tchounwou, 2014). The ongoing chain reactions result in MDA disrupting the structure of cellular enzymes, including those of the antioxidant system, thereby reducing their activity (Zhou et al., 2022). Nrf2, a key regulator of cellular antioxidant responses, is subject to release from Kelch like ECH associated protein 1 and activation of its target genes under OS conditions, and translocation to the nucleus. It plays an important role in counteracting OS by means of increased expression of antioxidant genes, such as HO-1, NQO-1, SOD and GPx (Ebrahimi et al., 2025). Recent research has emphasised the significance of CIS-induced ROS production, which suppresses the Nrf2 pathway and renders cells susceptible to CIS-related OS (Zhou et al., 2022; Mashayekhi-Sardoo et al., 2025). In line with this information, our results showed that the Nrf2 pathway was suppressed in the CIS group rats, resulting in high LPO and TOS levels. Conversely, elevated levels of Nrf2 and crucial components of the antioxidant system in the ovary were observed in response to high-dose UA treatment. The eradication of CIS-induced OS findings by UA can be regarded as an *in vivo* consequence of its radical scavenging activity, a property that has been previously substantiated in various models (Zhao et al., 2021). Additionally, previous experimental reports have demonstrated the potential of UA to modulate the Nrf2 pathway, which is consistent with our results (Fernández-Moriano et al., 2017; Demir et al., 2025).

Inflammation is one of the primary processes suggested for the toxic impact of CIS (Zhou et al., 2022). HMGB1, which is located in the nucleus and plays a role in chromosomal organisation, is a protein that is released outside the cell in cases of inflammation and acts as an alarmin (Yang et al., 2020). Extracellular HMGB1 causes activation of NF-κB signalling by binding to Toll like receptor 4 and/or Receptor for advanced glycation end-products receptors, which in turn leads to an increase in pro-inflammatory cytokines, including TNF-α (Yuan et al., 2024). Therefore, inhibiting the HMGB1/NF-κB/TNF-α axis is key to preventing tissue destruction caused by chronic inflammation (Ayazoglu Demir, 2024). Our findings indicated that the HMGB1/NF-κB/TNF-α axis was stimulated in the ovarian tissue of CIS-treated rats, exacerbating the leukocyte infiltration that was typified by elevated MPO. These results were similar to other reports that said that inflammation might play a role in injury models related to CIS (Mohamed et al., 2020; Zhou et al., 2022; Ayazoglu Demir et al., 2023). In contrast, significant

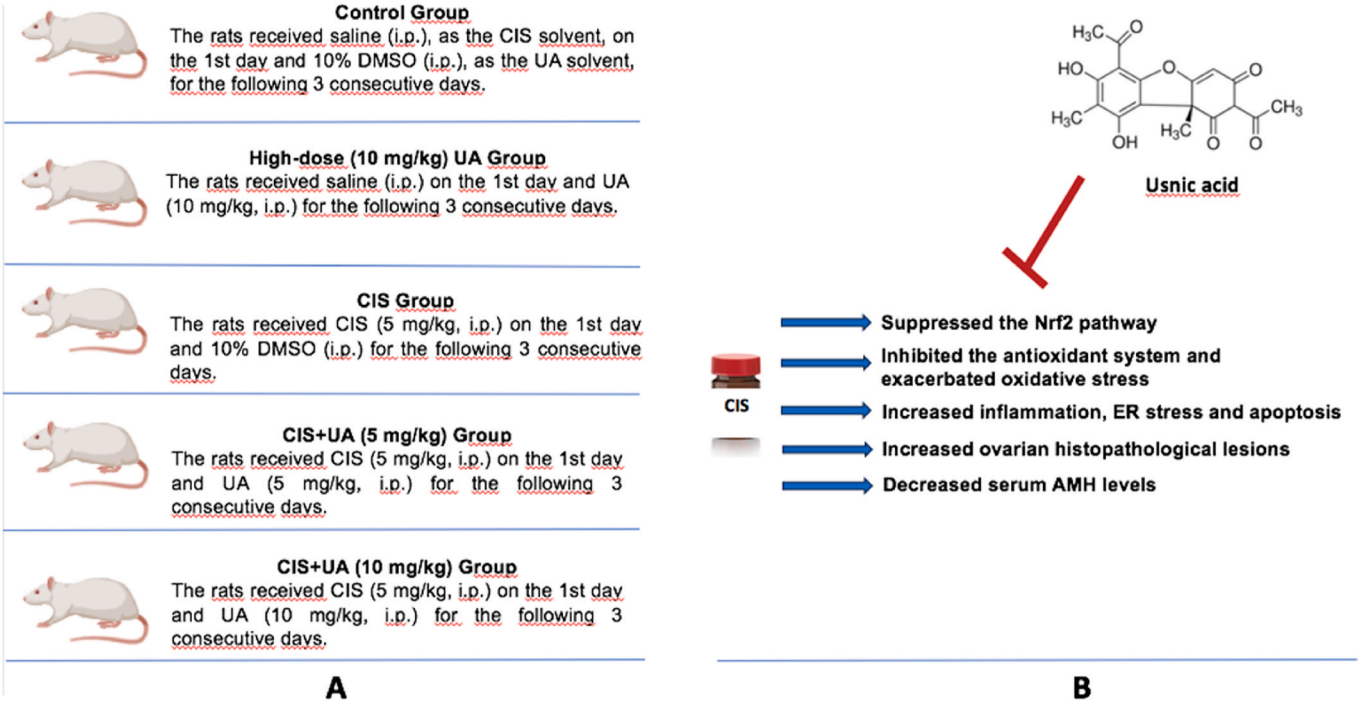


Fig. 4. A schematic summary of the experimental design (A) and key findings (B) of the study.

improvement in ovarian inflammation was seen with UA treatments (especially at the dose of 10 mg/kg). Nrf2 is one of the most important negative regulators of NF-κB, and its anti-inflammatory activity is derived from this negative regulatory feature (Ebrahimi et al., 2025). Confirming this mechanism, decreased Nrf2 levels were obtained in the CIS group, in contrast to increased NF-κB levels. In addition, improvement in ovarian inflammation levels may have been achieved by UA through its *in vivo* anti-inflammatory activity and Nrf2 modulatory activity. Consistent with our results, previous reports have emphasised the *in vivo* anti-inflammatory potential of UA (Paździora et al., 2023).

Reduced ability to fold ER proteins due to factors such as redox imbalance, inflammation, nutrient and ATP deficiency eventually leads to the accumulation of unfolded proteins in the ER lumen and ERS, which is characterised by ER dysfunction (Mozzini et al., 2017). A number of sensor proteins, including ATF6, detect the precipitated nonfunctional proteins in the ER lumen, prompting the cell to activate the unfolded protein response (UPR) pathway to restore ER homeostasis (Mashayekhi-Sardoo et al., 2025). Cell survival under mild ERS conditions is promoted by UPR activation, but under chronic and severe ERS conditions, the activation of transcriptional activities that promote apoptosis is initiated (Raudenska et al., 2019). BİP is an ER chaperone that normally keeps ATF6 inactive. When the UPR is activated in response to increased ERS, the interaction between BİP and ATF6 is disrupted (Mashayekhi-Sardoo et al., 2025). ATF6 is released from BİP and is transported to the Golgi, where it is cleaved and activated. Then it migrates to the nucleus, where the expression of genes that will restore proteostasis is induced (Mozzini et al., 2017). If ER proteostasis cannot be restored, ER-associated apoptosis is initiated by ATF6 by increasing the expression of GADD153, which can change the Bax/Bcl-2 ratio (Raudenska et al., 2019). The role of ERS and ERS-driven apoptosis in the toxic effects of CIS has been highlighted by recent evidence (Mashayekhi-Sardoo et al., 2025). As was the case with these studies, our research showed that CIS treatment made ERS and apoptosis in rat ovaries worse. Conversely, UA treatments eradicated CIS-induced ERS and apoptosis in a dose-dependent manner. It is known that Nrf2 controls the expression of components of the proteasomal ER-associated degradation system, which is activated under increased ERS conditions and relieves ER protein load (Raudenska et al., 2019). The observations of heightened ERS and apoptosis in the CIS group, in contradistinction to the repressed Nrf2 pathway, substantiate this inference. In addition, improvement in ovarian ERS and apoptosis levels may have been achieved by UA through its *in vivo* antioxidant activity and Nrf2 modulatory activity. Consistent with our results, previous reports have emphasised the potential of UA to inhibit ERS and ERS-induced apoptosis (Li et al., 2014; Demir et al., 2025).

It should be noted that there may be some limitations to our study. Firstly, as demonstrated in the fourteen-day acute toxicity studies, the administration of UA at doses of 100 and 200 mg/kg/day has been observed to induce hepatotoxic effects in rodents. However, lower doses have been reported to be well tolerated (Guo et al., 2008). Thus, relatively low doses of UA, which have previously been shown to exhibit beneficial biological activity (Yang et al., 2018; Lee et al., 2020; Demir et al., 2025) were selected for this study. The therapeutic effect of UA with gradual dose escalation can be re-examined in future studies. Secondly, the chemopreventive effect of UA against CIS-induced ovotoxicity was evaluated over a period of five days. Further studies should test the effectiveness of combinations of chronic CIS administration with different UA concentrations. Thirdly, the majority of the biochemical measurements conducted within the scope of this study were performed using commercial kits based on the ELISA method, owing to inadequate infrastructure and funding. In future studies, the ovoprotective efficacy of UA should be evaluated using detailed signalling investigations with molecular methods such as RT-PCR, Western blot, and/or immunohistochemistry. Fourthly, in this study, the ovarian reserve of the animals was assessed using AMH levels, an indirect indicator. However, given the limitations of AMH levels as a standalone indicator of ovarian function or fertility status, future studies should incorporate additional hormones associated with fertility, antral follicle count, and ovarian volume parameters to enhance the reliability of the assessment. Fifthly, although the chemopreventive effect of UA was tested biochemically and histologically, it was not possible to evaluate the effects of the treatments on the physiological sexual behaviour of female rats. In future studies, the effectiveness of UA should be examined using physiological behaviour models.

5. Conclusion

The present study is the first to offer a mechanistic understanding of the potential therapeutic impact of UA in a CIS-induced experimental model of oxidative and inflammatory ovarian damage. The findings indicate that the administration of UA, particularly at a dosage of 10 mg/kg, promotes the ovarian antioxidant system, thereby attenuating levels of OS, inflammation, ERS, and apoptosis. It is also suggested that this effect may be at least partially due to the reversal of CIS-induced inhibition of the Nrf2/HO-1 pathway by UA. These findings represent the first evidence that UA could serve as a promising protective molecule against the toxic effects of CIS. However, robust biochemical and physiological experimental studies supported by more comprehensive molecular techniques are needed before UA can be recommended for clinical use.

CRediT authorship contribution statement

Selim Demir: Writing – original draft, Project administration, Methodology, Funding acquisition, Formal analysis, Conceptualization. **Nihal Turkmen Alemdar:** Writing – original draft, Investigation, Formal analysis. **Ayten Livaoglu:** Methodology, Investigation. **Elif Ayazoglu Demir:** Investigation, Formal analysis. **Huseyin Yaman:** Software, Investigation. **Ahmet Mentese:** Supervision, Software, Conceptualization. **Yuksel Aliyazicioglu:** Writing – review & editing, Methodology.

Ethical approval

All procedures for animal experimentation were approved by the Animal Research Ethic Committee of Karadeniz Technical University (Approval number: 2021/48) and conducted precisely to the Directive 2010/63/EU and ARRIVE guideline.

Data availability

All data generated or analyzed during this study are included in this published article.

Funding

This study was supported by Office of Scientific Research Projects of Karadeniz Technical University (Türkiye) (Project number: TSA-2022-9828).

Declaration of competing interest

The authors declare that they have no known competing financial interests or personal relationships that could have appeared to influence the work reported in this paper.

Abbreviations

AMH: anti-mullerian hormone, ATF6: activating transcription factor 6, Bax: Bcl-2-like protein 4, Bcl-2: B cell lymphoma 2, BİP: binding immunoglobulin protein, CASP3: cleaved caspase-3, CIS: cisplatin, DMSO: dimethyl sulfoxide, ELISA: enzyme-linked immunosorbent

assay, ERS: endoplasmic reticulum stress, GADD153: growth arrest and DNA damage-inducible gene 153, GPx: glutathione peroxidase, GSH: glutathione, H&E: hematoxylin and eosin, HMGB1: high-mobility group box 1, HO-1: heme oxygenase-1, LPO: lipid peroxidation, MDA: malondialdehyde, MPO: myeloperoxidase, NF-κB: nuclear factor kappa B p65, NQO-1: NAD(P)H:quinone oxidoreductase-1, Nrf2: nuclear factor erythroid 2-related factor 2, OS: oxidative stress, ROS: reactive oxygen species, SEM: standard error of the mean, SOD: superoxide dismutase, TNF-α: tumor necrosis factor-alpha, TOS: total oxidant status, UA: usnic acid; UPR: unfolded protein response.

References

Aksoy, A.N., Kabil Kucur, S., Batmaz, G., Gözükara, I., Aksoy, M., Kurt, N., et al., 2015. The role of antioxidant activity in the prevention and treatment of infertility caused by cisplatin in rats. Gynecol. Obstet. Invest. 79 (2), 119–125. https://doi.org/10.1159/000367657.

Atli, M., Engin-Ustun, Y., Tokmak, A., Caydere, M., Hucumenoglu, S., Topcuoglu, C., 2017. Dose dependent effect of resveratrol in preventing cisplatin-induced ovarian damage in rats: an experimental study. Reprod. Biol. 17 (3), 274–280. https://doi.org/10.1016/j.repbio.2017.07.001.

Ayazoglu Demir, E., 2024. Syringic acid alleviates cisplatin-induced ovarian injury through modulating endoplasmic reticulum stress, inflammation and Nrf2 pathway. J. Trace Elem. Med. Biol. 82, 127356. https://doi.org/10.1016/j.jtemb.2023.127356.

Ayazoglu Demir, E., Mentese, A., Yilmaz, Z.S., Alemdar, N.T., Demir, S., Aliyazicioglu, Y., 2023. Evaluation of the therapeutic effects of arbutin on cisplatin-induced ovarian toxicity in rats through endoplasmic reticulum stress and Nrf2 pathway. Reprod. Biol. 23 (4), 100824. https://doi.org/10.1016/j.repbio.2023.100824.

Bhardwaj, J.K., Bikal, P., Sachdeva, S.N., 2023. Chemotherapeutic drugs induced female reproductive toxicity and treatment strategies. J. Biochem. Mol. Toxicol. 37 (7), e23371. https://doi.org/10.1016/10.1002/jbt.23371.

Borovskaya, T.G., Goldberg, V.E., Fomina, T.I., Pakhomova, A.V., Kseneva, S.I., Poluektova, M.E., et al., 2004. Morphological and functional state of rat ovaries in early and late periods after administration of platinum cytostatics. Bull. Exp. Biol. Med. 137 (4), 331–335. https://doi.org/10.1023/b:bebm.0000035121.85533.08.

Calcott, M.J., Ackerley, D.F., Knight, A., Keyzers, R.A., Owen, J.G., 2018. Secondary metabolism in the lichen symbiosis. Chem. Soc. Rev. 47 (5), 1730–1760. https://doi.org/10.1039/c7cs00431a.

Dasari, S., Tchounwou, P.B., 2014. Cisplatin in cancer therapy: molecular mechanisms of action. Eur. J. Pharmacol. 740, 364–378. https://doi.org/10.1016/j.ejphar.2014.07.025.

Demir, S., Alemdar, N.T., Yulug, E., Demir, E.A., Durmus, T.B., Mentese, A., et al., 2025. Usnic acid suppresses inflammation and endoplasmic reticulum stress in a methotrexate-induced pulmonary toxicity model via modulating Nrf2 pathway. S. Afr. J. Bot. 177, 572–578. https://doi.org/10.1016/j.sajb.2024.12.036.

Demir, S., Kazaz, I.O., Mungan, S.A., Alemdar, N.T., Perolli, N., Demir, E.A., et al., 2024a. Usnic acid alleviates testicular ischemia/reperfusion injury in rats by modulating endoplasmic reticulum stress. Reprod. Toxicol. 128, 108654. https://doi.org/10.1016/j.reprotox.2024.108654.

Demir, S., Mentese, A., Kucuk, H., Yulug, E., Alemdar, N.T., Demir, E.A., et al., 2024b. Ethyl pyruvate attenuates cisplatin-induced ovarian injury in rats via activating Nrf2 pathway. Drug Chem. Toxicol. 47 (2), 218–226. https://doi.org/10.1080/01480545.2023.2217481.

Ebrahimi, R., Mohammadpour, A., Medoro, A., Davinelli, S., Saso, L., Miroliaei, M., 2025. Exploring the links between polyphenols, Nrf2, and diabetes: a review. Biomed. Pharmacother. 186, 118020. https://doi.org/10.1016/j.biopha.2025.118020.

Fernández-Moriano, C., Divakar, P.K., Crespo, A., Gómez-Serranillos, M.P., 2017. Protective effects of lichen metabolites evernic and usnic acids against redox impairment-mediated cytotoxicity in central nervous system-like cells. Food Chem. Toxicol. 105, 262–277. https://doi.org/10.1016/j.fct.2017.04.030.

Guo, L., Shi, Q., Fang, J.L., Mei, N., Ali, A.A., Lewis, S.M., Leakey, J.E., Frankos, V.H., 2008. Review of usnic acid and *Usnea barbata* toxicity. J. Environ. Sci. Health C Environ. Carcinog. Ecotoxicol. Rev. 26 (4), 317–338. https://doi.org/10.1080/10590500802533392.

Huang, W., Zhong, Y., Gao, B., Zheng, B., Liu, Y., 2023. Nrf2-mediated therapeutic effects of dietary flavones in different diseases. Front. Pharmacol. 14, 1240433. https://doi.org/10.3389/fphar.2023.

Kaygusuzoglu, E., Caglayan, C., Kandemir, F.M., Yıldırım, S., Kucukler, S., Kılınc, M.A., et al., 2018. Zingerone ameliorates cisplatin-induced ovarian and uterine toxicity via suppression of sex hormone imbalances, oxidative stress, inflammation and apoptosis in female wistar rats. Biomed. Pharmacother. 102, 517–530. https://doi.org/10.1016/j.biopha.2018.03.119.

Lee, S., Lee, Y., Ha, S., Chung, H.Y., Kim, H., Hur, J.S., et al., 2020. Anti-inflammatory effects of usnic acid in an MPTP-induced mouse model of Parkinson's disease. Brain Res. 1730, 146642. https://doi.org/10.1016/j.brainres.2019.146642.

Li, F., Zhu, F., Wang, S., Hu, H., Zhang, D., He, Z., et al., 2024. Icariin alleviates cisplatin-induced premature ovarian failure by inhibiting ferroptosis through activation of the Nrf2/ARE pathway. Sci. Rep. 14 (1), 17318. https://doi.org/10.1038/s41598-024-67557-x.

Li, J., Di, L.H., Liu, W.X., Ren, Y.L., 2014. Usnic acid inhibits ER stress activation through AMPK signaling pathway in rat cardiomyocytes. Eur. Rev. Med. Pharmacol. Sci. 18 (17), 2538–2543.

Mashayekhi-Sardoo, H., Rezaee, R., Yarmohammadi, F., Karimi, G., 2025. Targeting endoplasmic reticulum stress by natural and chemical compounds ameliorates cisplatin-induced nephrotoxicity: a review. Biol. Trace Elem. Res. 203 (5), 2687–2700. https://doi.org/10.1007/s12011-024-04351-w.

Mentese, A., Alemdar, N.T., Livaoglu, A., Ayazoglu Demir, E., Aliyazicioglu, Y., Demir, S., 2022. Suppression of cisplatin-induced ovarian injury in rats by chrysin: an experimental study. J. Obstet. Gynaecol. 42 (8), 3584–3590. https://doi.org/10.1080/01443615.2022.2130201.

Mentese, U., Dogan, O.V., Turan, I., Usta, S., Dogan, E., Mentese, S.O., et al., 2014. Oxidant-antioxidant balance during on-pump coronary artery bypass grafting. Sci. World J. 2014, 263058. https://doi.org/10.1155/2014/263058.

Mihara, M., Uchiyama, M., 1978. Determination of malonaldehyde precursor in tissues by thiobarbituric acid test. Anal. Biochem. 86 (1), 271–278. https://doi.org/10.1016/0003-2697(78)90342-1.

Mohamed, M.E., Abduldaium, Y.S., Younis, N.S., 2020. Ameliorative effect of linalool in cisplatin-induced nephrotoxicity: the role of HMGB1/TLR4/NF-κB and Nrf2/HO1 pathways. Biomolecules 10 (11), 1488. https://doi.org/10.3390/biom10111488.

Morgan, S., Anderson, R.A., Gourley, C., Wallace, W.H., Spears, N., 2012. How do chemotherapeutic agents damage the ovary? Hum. Reprod. Update 18 (5), 525–535. https://doi.org/10.1093/humupd/dms022.

Mozzini, C., Cominacini, L., Garbin, U., Fratta Pasini, A.M., 2017. Endoplasmic reticulum stress, Nrf2 signalling and cardiovascular diseases in a nutshell. Curr. Atheroscler. Rep. 19 (8), 33. https://doi.org/10.1007/s11883-017-0669-7.

Muttukrishna, S., McGarrigle, H., Wakim, R., Khadum, I., Ranieri, D.M., Serhal, P., 2005. Antral follicle count, Anti-mullerian hormone and inhibin B: predictors of ovarian response in assisted reproductive technology? BJOG 112 (10), 1384–1390. https://doi.org/10.1111/j.1471-0528.2005.00670.x.

Odabasoglu, F., Cakir, A., Suleyman, H., Aslan, A., Bayir, Y., Halici, M., et al., 2006. Gastroprotective and antioxidant effects of usnic acid on indomethacin-induced gastric ulcer in rats. J. Ethnopharmacol. 103 (1), 59–65. https://doi.org/10.1016/j.jep.2005.06.043.

Özcan, P., Fıçıcıoğlu, C., Yıldırım, Ö.K., Özkan, F., Akkaya, H., Aslan, İ., 2015. Protective effect of resveratrol against oxidative damage to ovarian reserve in female Sprague-Dawley rats. Reprod. Biomed. Online 31 (3), 404–410. https://doi.org/10.1016/j.rbmo.2015.06.007.

Paździora, W., Podolak, I., Grudzińska, M., Paśko, P., Grabowska, K., Galanty, A., 2023. Critical assessment of the anti-inflammatory potential of usnic acid and its derivatives-A review. Life 13 (4), 1046. https://doi.org/10.3390/life13041046.

Raudenska, M., Balvan, J., Fojtu, M., Gumulec, J., Masarik, M., 2019. Unexpected therapeutic effects of cisplatin. Metallomics 11 (7), 1182–1199. https://doi.org/10.1039/c9mt00049f.

Smith, P.K., Krohn, R.I., Hermanson, G.T., Mallia, A.K., Gartner, F.H., Provenzano, M.D., et al., 1985. Measurement of protein using bicinchoninic acid. Anal. Biochem. 150 (1), 76–85. https://doi.org/10.1016/0003-2697(85)90442-7.

Yang, H., Wang, H., Andersson, U., 2020. Targeting inflammation driven by HMGB1. Front. Immunol. 11, 484. https://doi.org/10.3389/fimmu.2020.00484.

Yang, Y., Bae, W.K., Lee, J.Y., Choi, Y.J., Lee, K.H., Park, M.S., Yu, Y.H., Park, S.Y., Zhou, R., Taş, İ., Gamage, C., Paik, M.J., Lee, J.H., Chung, I.J., Kim, K.K., Hur, J.S., Kim, S.K., Ha, H.H., Kim, H., 2018. Potassium usnate, a water-soluble usnic acid salt, shows enhanced bioavailability and inhibits invasion and metastasis in colorectal cancer. Sci. Rep. 8 (1), 16234. https://doi.org/10.1038/s41598-018-34709-9.

Yeh, J., Kim, B., Liang, Y.J., Peresie, J., 2006. Müllerian inhibiting substance as a novel biomarker of cisplatin-induced ovarian damage. Biochem. Biophys. Res. Commun. 348 (2), 337–344. https://doi.org/10.1016/j.bbrc.2006.06.195.

Yuan, J., Guo, L., Ma, J., Zhang, H., Xiao, M., Li, N., et al., 2024. HMGB1 as an extracellular pro-inflammatory cytokine: implications for drug-induced organic damage. Cell Biol. Toxicol. 40 (1), 55. https://doi.org/10.1007/s10565-024-09893-2.

Yuluğ, E., Türedi, S., Yıldırım, Ö., Yenilmez, E., Aliyazıcıoğlu, Y., Demir, S., et al., 2019. Biochemical and morphological evaluation of the effects of propolis on cisplatin induced kidney damage in rats. Biotech. Histochem. 94 (3), 204–213. https://doi.org/10.1080/10520295.2018.1543895.

Zhao, Y., Wang, M., Xu, B., 2021. A comprehensive review on secondary metabolites and health-promoting effects of edible lichen. J. Funct.Foods 80, 104283. https://doi.org/10.1016/j.jff.2020.104283.

Zhou, J., Nie, R.C., Yin, Y.X., Cai, X.X., Xie, D., Cai, M.Y., 2022. Protective effect of natural antioxidants on reducing cisplatin-induced nephrotoxicity. Dis. Markers 2022, 1612348. https://doi.org/10.1155/2022/1612348.